

# Monte Carlo simulations disambiguate the biophysical mechanisms of diffusion hindrance along tracts

Submission Number:

6096

Submission Type:

Abstract Submission

Authors:

Michiel Kleinnijenhuis<sup>1</sup>, Jeroen Mollink<sup>1</sup>, Paul Kinchesh<sup>2</sup>, Wilfred Lam<sup>1</sup>, Alexandre Khrapitchev<sup>2</sup>, Nicola Sibson<sup>2</sup>, Vitaly Galinsky<sup>3</sup>, Lawrence Frank<sup>3</sup>, Sean Smart<sup>2</sup>, Saad Jbabdi<sup>1</sup>, Karla Miller<sup>1</sup>

Institutions:

<sup>1</sup>FMRIB Centre, University of Oxford, Oxford, United Kingdom, <sup>2</sup>CR-UK & MRC Oxford Institute for Radiation Oncology, Department of Oncology, University of Oxford, Oxford, United Kingdom, <sup>3</sup>Center for Scientific Computation in Imaging, University of California San Diego, La Jolla, CA

Introduction:

Diffusion imaging at long diffusion times can inform on microstructural features of tissue spanning several hundreds of micrometers. At these scales the approximation of axons as straight cylinders might not hold, even for tissues that are generally assumed to be coherently organized. For example, the human corpus callosum (CC) is often used as a reference structure for simple fibre configuration. Nevertheless, electron microscopy (Mikula 2012) and histology (Budde 2013) suggest that the CC is far from coherent. Fibres bend, twist and undulate along the tract which might lead to specific signatures of hindrance "along" the tract. In this study, we investigated the diffusion time dependence of the apparent diffusion coefficient (ADC) along the fibres in the CC. Biophysical mechanisms of this dependence are explored by Monte Carlo simulations of various axon models.

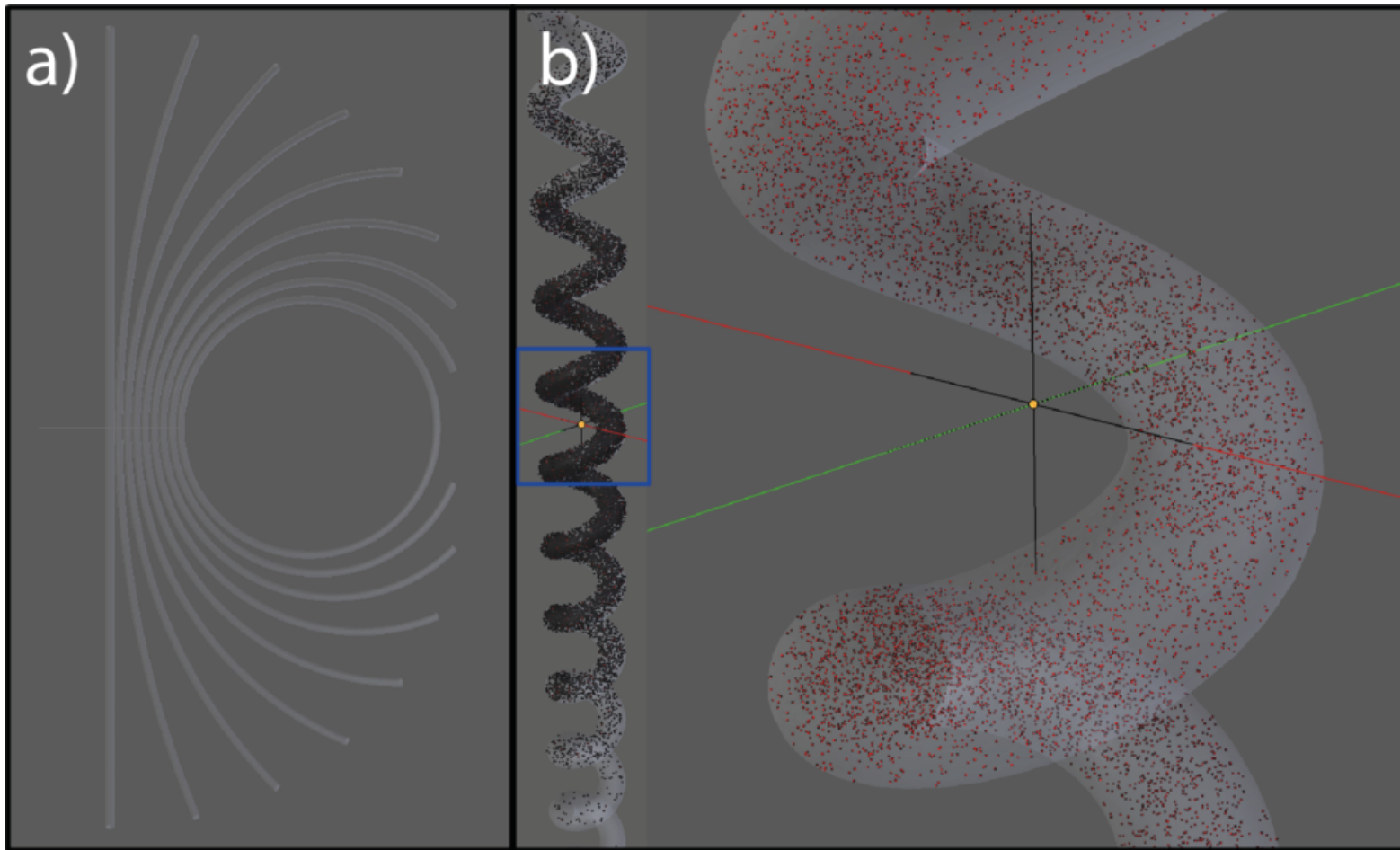


**Figure 1.** Simulated geometries. a) fanning and bending - each individual axon represents one of the bending geometries, the set forms the fanning geometry. b) undulating: helical geometry with molecules diffusing intracellularly. Axon models were created in Blender with CellBlender plugin for compatibility with diffusion-reaction simulator MCell (Stiles 1996) used by DifSim.

Methods:

A 3x2 cm block of a fixed human CC was cut from a 5 mm thick coronal slice at the level of the anterior commissure. It was soaked in PBS for 72h and scanned in a syringe with Fluorinert (3M) on a Varian 9.4T MRI system. Diffusion-weighted STEAM data were acquired with diffusion gradients ( $\delta=2.22$  ms) applied in 30 directions for 9 mixing times ([24.3,59.3,89.3,139.3,189.3,239.3,289.3,339.3,389.3] ms) with a fixed q-value (0.14 rad/ $\mu$ m). Imaging parameters: 10 slices of 400  $\mu$ m isotropic voxels, TE=16ms, TR=2.4-4.1s. Spin-echo diffusion data were acquired with TR/TE=2.4s/29ms, 240 directions ( $\delta=6$ ms,  $\Delta=16$ ms) with  $b=[2500,5000]$  s\*mm<sup>-2</sup>. Diffusion MR signal attenuation was calculated for the same protocols as used in the postmortem MRI protocols with Monte Carlo diffusion MR simulator DifSim (Balls 2009) for axon models with various degrees of bending, fanning and undulation. Axons of 5  $\mu$ m radius with length [.5,1,2] mm were bent over [0,45,...,360] $^{\circ}$  (Figure 1). Fanning configurations were created by taking the set of bending axons of a given length. Undulations were modeled as helices (radius=5  $\mu$ m; amplitude=1.5  $\mu$ m; length=2 mm) with [30,50,70,90] turns. In each model, 9600 molecules were released at t=0  $\mu$ s from the plane bisecting the model. Simulation parameters: T=402400  $\mu$ s, dt=1  $\mu$ s; d=2  $\mu$ m<sup>2</sup>/ms). Note that in a previous report on these simulations (Kleinnijenhuis 2015) the spatial scale was reported incorrectly.

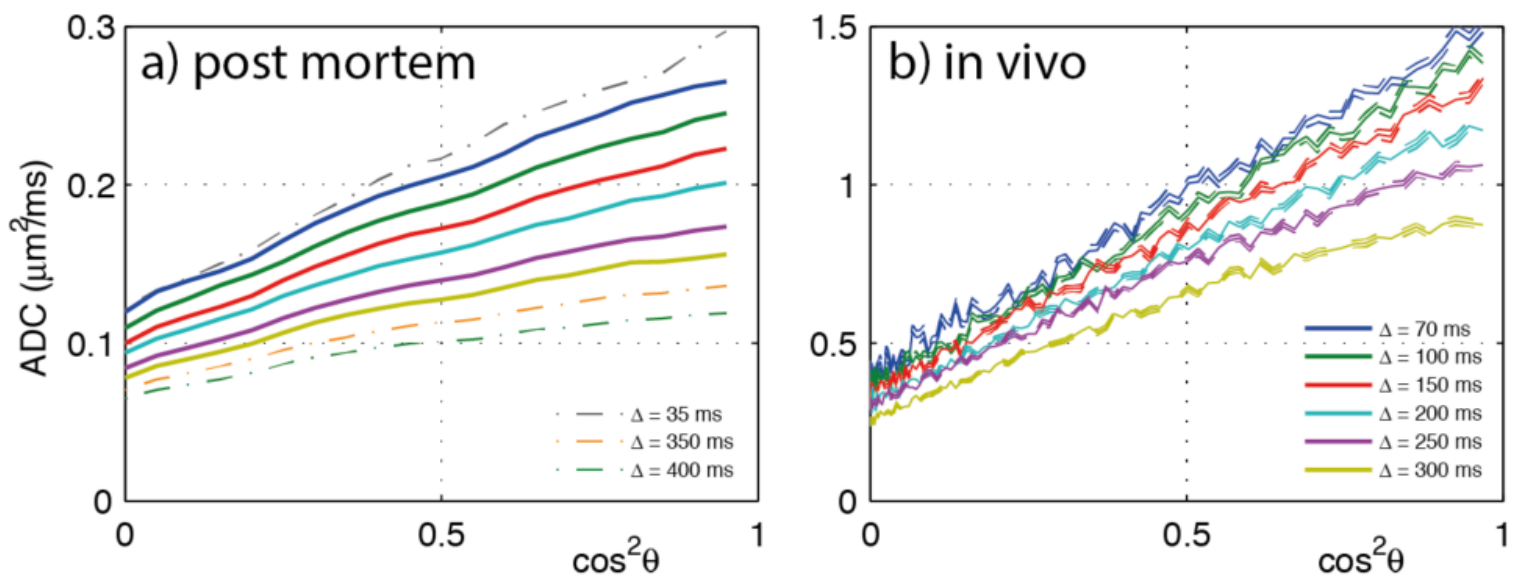


**Figure 2.** ADC plotted against the  $\cos^2$  of the angle between the diffusion gradient and the primary diffusion direction. Similar patterns are seen for post mortem and in vivo data. Diffusion time dependence is seen perpendicular to the main fibre directions, but ADC also varies strongly with diffusion time along the fibres.

### Results:

Figure 2 demonstrates diffusion time dependence of the ADC for different orientations of the fibre ( $\cos^2\theta$ , from a tensor fit to the SE-DWI). Post mortem (Figure 2a) and in vivo data (Figure 2b; Lam 2015) show decreasing ADC at longer diffusion times due to some source of hindrance. This is observed perpendicular to the axons ( $\cos^2\theta=0$ ), but also along the fibre direction ( $\cos^2\theta=1$ ). Bending, fanning and undulating (Figure 1) were investigated as potential sources of the hindrance. Simulation results are summarized in Figure 3, where the ADC along the tract is plotted vs. diffusion time for simulations and post mortem data. Slightly bending axons (panel A, blue lines:  $< \sim 2^\circ/\mu\text{m}$ ) show little sign of hindrance. Axons with sharper bends ( $\sim 5\text{--}6^\circ/\mu\text{m}$ ) match the observed slope and shape of the curve better. The fanning pattern (B) of the short axons shows behaviour similar to the sharper bending geometries suggesting that fibre fanning could also explain the data. The undulation (C), however, is inconsistent with the data: no diffusion time dependence was observed at long diffusion time (see Nilsson 2012).

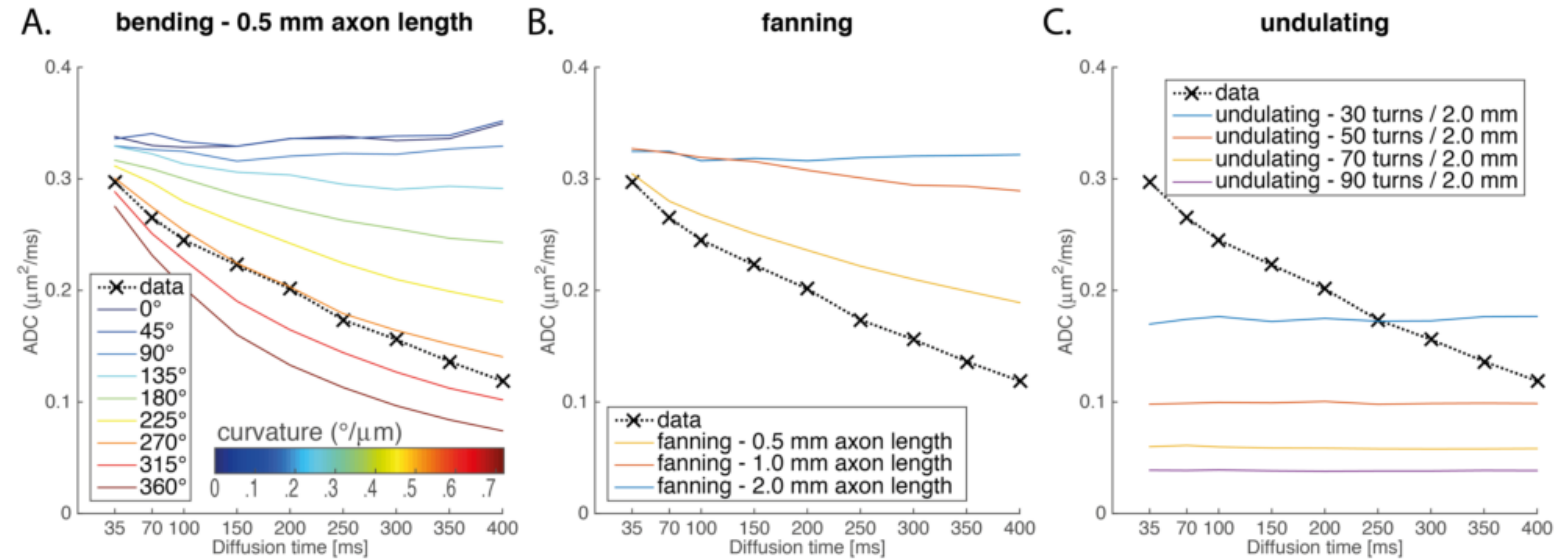


**Figure 3.** Comparison between post mortem ADC along the fibre direction of the corpus callosum (black x's) and simulation results. As the true free diffusion coefficient of intracellular space is unknown and different for the in vivo and post mortem case, all simulation results are scaled to provide the best match with the data. This is for the 0.5 mm axon model bent over  $270^\circ$  (panel A;  $0.54^\circ/\mu\text{m}$ ). Gentle bending (panel A, blue lines), gentle fanning (panel B, blue line) and undulation (panel C) do not produce the pattern of decreasing ADC with diffusion time. Line colors in panel A represent the curvature of the bends. Simulation results of bending axons of 1.0 and 2.0 mm are not shown, as they overlap with the lower curvature regime of the 0.5 mm axon and results were found to be similar. The longer axons were included in the experiment to simulate various degrees of fanning as well as to confirm that the effects did not originate from molecules possibly hitting the boundaries at the long ends of the axons (the average diffusion distance at the longest diffusion time is  $\sim 40 \mu\text{m}$ ).

### Conclusions:

Diffusion along axonal tracts exhibits hindrance at long diffusion times. This effect could be used as a means to derive information about the microscopic anatomy within fibre bundles. Simulations suggest that one of the causes for restricted diffusion along fibres might be bending or fanning of axons, but that bends at a particular scale are required to induce the observed relation between diffusion time and ADC. The plausibility of such configurations in the CC should be quantified in future histological investigations.

### Imaging Methods:

Modeling and Analysis Methods:

Diffusion MRI Modeling and Analysis <sup>2</sup>

Keywords:

- Cellular
- Modeling
- MRI
- MRI PHYSICS
- Neuron
- White Matter
- WHITE MATTER IMAGING - DTI, HARDI, DSI, ETC
- Other - Monte Carlo simulations

<sup>1|2</sup>Indicates the priority used for review

Would you accept an oral presentation if your abstract is selected for an oral session?

Yes

Please indicate below if your study was a "resting state" or "task-activation" study.

Other

Healthy subjects only or patients (note that patient studies may also involve healthy subjects):

Healthy subjects

Internal Review Board (IRB) or Animal Use and Care Committee (AUCC) Approval. Please indicate approval below. Please note: Failure to have IRB or AUCC approval, if applicable will lead to automatic rejection of abstract.

Not applicable

Please indicate which methods were used in your research:

- Diffusion MRI
- Postmortem anatomy
- Other, Please specify - monte carlo simulation

Which processing packages did you use for your study?

FSL

Provide references in author date format

Balls, G.T. (2009), 'A simulation environment for diffusion weighted MR experiments in complex media', Magnetic Resonance in Medicine, vol. 62, no. 3, pp.771-8.

Budde, M.D. (2013), 'Quantification of anisotropy and fiber orientation in human brain histological sections', Frontiers in Integrative Neuroscience, vol. 7, pp. 1-8.

Kleinnijenhuis, M., 'Monte Carlo diffusion simulations disambiguate the biophysical mechanisms of diffusion hinderance along tracts', Proceedings of the Society for Magnetic Resonance in Medicine, 2015.

Lam, W.W. 2015, 'Quantification of Microscopic Brain Structures Using Diffusion Magnetic Resonance', PhD thesis, 2015.

Mikula, S. (2012), 'Staining and embedding the whole mouse brain for electron microscopy', Nature Methods, vol. 9, no. 12, pp. 1198-201.

Nilsson, M. (2012), 'The importance of axonal undulation in diffusion MR measurements: a Monte Carlo simulation study', NMR in Biomedicine, vol. 25, no. 5, pp. 795-805.

Stiles, J.R. (1996), 'Miniature endplate current rise times less than 100 microseconds from improved dual recordings can be modeled with passive acetylcholine diffusion from a synaptic vesicle', Proceedings of the National Academy of Sciences of the United States of America, vol. 93, no. 12, pp. 5747-52.

ACKNOWLEDGEMENTS – Funded by Wellcome Trust. Thanks to Dave Flitney for help with simulations.